Korean J. Chem. Eng., **31**(11), 1919-1934 (2014)
DOI: 10.1007/s11814-014-0257-2
pISSN: 0256-1115
eISSN: 1975-7220

REVIEW PAPER

CO_2 capture by amine-functionalized nanoporous materials: A review

Chao Chen*,, Jun Kim*, and Wha-Seung Ahn*,†**

*Department of Chemistry and Chemical Engineering, Inha University, Incheon 402-751, Korea
**College of Chemistry and Chemical Engineering, Xinyang Normal University, Xinyang, Henan Province 464000, China
(*Received 27 April 2014 • accepted 1 September 2014*)

Abstract–Amine-functionalized nanoporous materials can be prepared by the incorporation of diverse organic amine moieties into the pore structures of a range of support materials, such as mesoporous silica and alumina, zeolite, carbon and metal organic frameworks (MOFs), either by direct functionalization or post-synthesis through physical impregnation or grafting. These hybrid materials have great potential for practical applications, such as dry adsorbents for post-combustion CO_2 capture, owing to their high CO_2 capture capacity, high capture selectivity towards CO_2 compared to other gases, and excellent stability. This paper summarizes the preparation methods and CO_2 capture performance based on the equilibrium CO_2 uptake of a range of amine-functionalized nanoporous materials.

Keywords: Amine-functionalization, CO_2 Capture, Impregnation, Grafting, Mesoporous Silica, Mesoporous Alumina, Zeolite, Carbon, Metal Organic Frameworks (MOFs), Porous Polymer

INTRODUCTION

The anthropogenic emissions of greenhouse gases are causing serious global problems. Among these gases, CO_2 contributes approximately 60% to the global warming effect [1]. The annual global emissions of CO_2 escalated by approximately 80% between 1970 and 2004, mainly by the combustion of fossil fuels. The CO_2 concentration in the atmosphere is still increasing, which has led to urgent calls for strategies to alleviate this problem. The International Energy Agency (IEA) suggests that by 2050 the global emissions of CO_2 from all energy-related technologies need to be reduced to half of their 2007 levels (29 Gt CO_2 per annum) to stabilize global warming [2].

Considerable effort has been focused over the last decade to develop a range of chemical and physical methods for efficient CO_2 capture and sequestration (CCS) [3]. Fig. 1 shows a variety of reported CO_2 sorbents. Currently, the large-scale separation of CO_2 by the liquid phase amine-based absorption process is in commercial operation throughout the world. This "wet-scrubbing" CO_2 capture utilizes alkanolamines, such as MEA (monoethanolamine), as the solvent, which has been used industrially over the past 50 years [4,5]. During the absorption process, amine molecules in aqueous solutions react with CO_2 to form water soluble compounds [6]. As shown in Fig. 2, 2 mol of amine species react with 1 mol CO_2 under dry conditions to form carbamates for primary and secondary amines, and the reaction stoichiometry changes to 1 : 1 in the presence of water to form hydrogen carbonate. Water is essential for tertiary amines in the CO_2 capture process, in which 1 mol of amine species

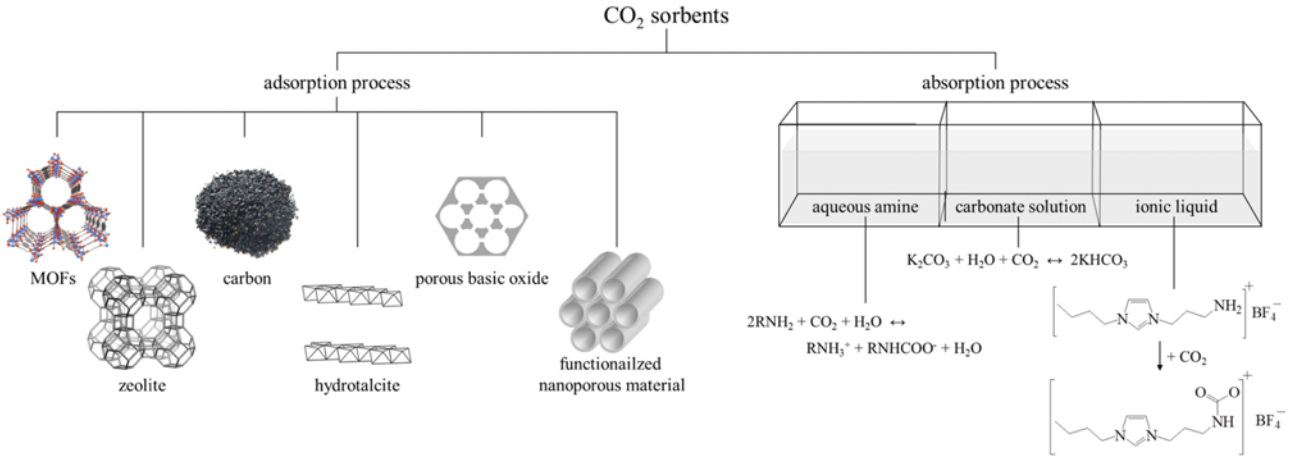

Fig. 1. CO_2 capture by sorption processes.

†To whom correspondence should be addressed.
E-mail: whasahn@inha.ac.kr

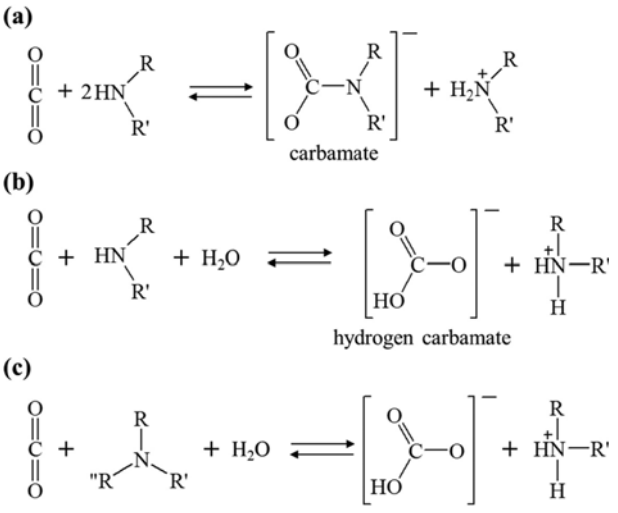

Fig. 2. General reaction schemes for the chemical absorption of CO_2 by primary or secondary amines (a) without water, (b) with water, and (c) tertiary amine-containing solvents [3].

reacts with 1 mol CO_2 to form hydrogen carbonate as the final product. An amine solution has higher capture selectivity to CO_2 than N_2 and the CO_2 capture capacity is not affected strongly by the CO_2 partial pressure. Therefore, amine-based systems can efficiently remove CO_2 from the flue gas of conventional pulverized coal-fired power plants. However, they also suffer a number of drawbacks, such as a large amount of energy required for solvent regeneration, equipment corrosion and solvent degradation in the presence of oxygen [7]. Other CO_2 sorbents based on various absorption processes include those using ammonia [8], soluble carbonate [9], or ionic liquids [10]. An ammonia-based system is similar in operation to amine systems and is absent from degradation during the absorption and regeneration process. Unfortunately, ammonia losses occur at elevated temperatures during the regeneration step. Carbonate systems are based on the ability of soluble carbonate to react with CO_2 to form bicarbonate. CO_2 capture by ionic liquids has been investigated mainly in academic laboratories, but the high cost of ionic liquids remains a problem for practical applications.

Compared to absorption technologies based on liquid solvents, adsorption is more energy-efficient in capturing CO_2 from flue gases [11]. CO_2 adsorption processes based on solid adsorbents, such as zeolites [12-18], activated carbon [19-21] and MOFs (metal organic frameworks) [22-28], have been investigated, which all have high surface areas for the effective physisorption of CO_2. These materials, however, are mainly applicable to low temperature applications

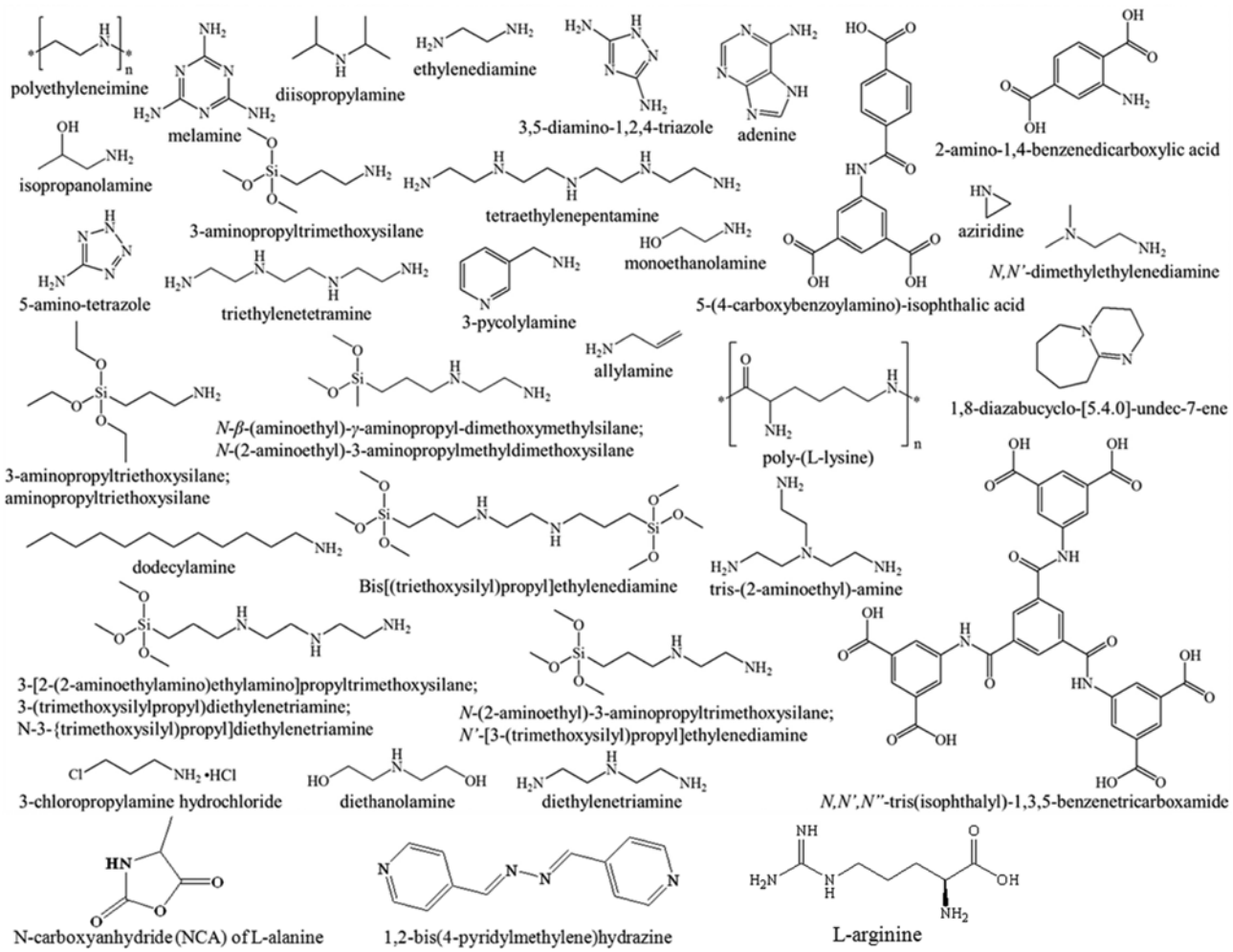

Fig. 3. Molecular structure of amine species used for the synthesis and functionalization of a range of nanoporous materials for CO_2 capture.

because a rapid decrease in capture capacity takes place with increasing temperature. The relatively low selectivity to CO_2 from combustion flue gases is another drawback. Basic oxide and hydrotalcite materials are capable of scavenging CO_2 at high temperatures [29-34], which normally capture CO_2 through chemical reactions with CO_2 to form carbonates. Most of these adsorbents, however, suffer from either low CO_2 capture capacities, energy penalties because of the high desorption temperature required, or the poor CO_2 capture performance in a cyclic process [33].

The CO_2 capture performance can be improved by introducing a functional group with affinity for CO_2 (e.g., amine group) into a structure of nanoporous material because the introduction of basic amine groups into pore structure of a nanoporous support can lead to a composite solid material with the preferential adsorption of weakly acidic CO_2. Fig. 3 shows the chemical structures of amine species employed for this purpose. These amine groups can be incorporated into a nanoporous material by direct functionalization, or post synthetically through physical impregnation or a chemical grafting method. The prepared composite material tends to combine the advantages of nanoporous support (large surface area and pore volume) and amine groups (high affinity for CO_2) by finely dispersing amine groups inside the nanoporous support, leading to 1) enhanced mass transfer, rapid adsorption kinetics and high CO_2 capture capacity, 2) high selectivity towards CO_2 due to the affinity of amine groups to CO_2, and 3) reduced energy requirements for sorbent regeneration.

In the last few years, several excellent review papers dealing with CO_2 capture and separation have been published [3,35] that provide a good perspective towards the progresses made on the topic. Review articles dealing with CO_2 capture specifically over the general solid adsorbents [36], nanoporous materials [11,37], MOFs [38], ionic liquids [10] and chemisorbents [33,39] have also appeared. In our opinion, a review focusing more specifically on the amine-functionalized nanoporous materials for CO_2 capture can be still useful, because amine-functionalization has been the universal con-

Table 1. CO_2 capture by amine-functionalized mesoporous silicas

Support material	Amine type	Temp. (°C)	CO_2 partial pressure (atm)	CO_2 adsorption capacity (mg/g)		Reference
				Dry CO_2	Humid CO_2	
MCM-41	Polyethylenimine	75	1	133	-	[43]
MCM-41	Polyethylenimine	75	0.005	48	-	[44]
MCM-41	Polyethylenimine	75	0.15	89	131	[45]
MCM-41	3-Aminopropyltriethoxysilane	20	1	47	-	[46]
MCM-41	N-β-(aminoethyl)-γ-aminopropyl dimethoxymethylsilane	25	1	97	-	[47]
MCM-41	Aminopropyltriethoxysilane	−10	20	581	-	[48]
MCM-41	Diisopropylamine	75	1	75	-	[49]
Pore expanded MCM-41	Diethanolamine	25	0.05	104	125	[50]
Pore expanded MCM-41	Polyethylenimine	75	1	210	-	[51]
Pore expanded MCM-41	3-[2-(2-Aminoethylamino) ethylamino] propyltrimethoxysilane	25	0.05	117	129	[52]
As-syn MCM-41	Triethylenetetramine	60	0.15	98	-	[53]
As-syn MCM-41	Tetraethylenepentamine	75	0.05	200	-	[54]
MCM-48	3-Aminopropyltriethoxysilane	25	0.05	50	100	[55]
MCM-48	3-Aminopropyltriethoxysilane	25	1	35	-	[56]
MCM-48	Tris(2-aminoethyl)amine	25	1	70	-	[57]
SBA-15	Polyethylenimine	75	0.15	105	-	[58]
SBA-15	Polyethylenimine	75	1	90	-	[59]
SBA-15	Polyethylenimine	75	1	173	-	[60]
SBA-15	3-Aminopropyltrimethoxysilane	25	0.15	70	-	[61]
SBA-15	3-Aminopropyltriethoxysilane	25	0.1	66	-	[62]
SBA-15	Ethylenediamine	22	1	86	-	[63]
SBA-15	(3-Trimethoxysilylpropyl) diethylenetriamine	60	0.15	70	79	[64]
SBA-15	(3-Trimethoxysilylpropyl) diethylenetriamine	60	0.15	106	120	[65]
SBA-15	Aziridine	25	0.0004	-	76	[66]
SBA-15	Aziridine	25	0.1	-	92	[67]
SBA-15	Poly-(L-lysine)	25	0.0004	26	-	[68]
SBA-15	Polyethylenimine	75	0.15	140	-	[69]
As-syn SBA-15	Tetraethylenepentamine	75	1	173	-	[70]

Table 1. Continued

Support material	Amine type	Temp. (°C)	CO_2 partial pressure (atm)	CO_2 adsorption capacity (mg/g)		Reference
				Dry CO_2	Humid CO_2	
SBA-16	N-(2-Aminoethyl)-3-aminopropyltrimethoxysilane	60	0.15	32	-	[71]
SBA-16	N′-[3-(Trimethoxysilyl)propyl] ethylenediamine	27	30	238	-	[72]
SBA-12	3-Aminopropyltrimethoxysilane	25	0.1	46		[73]
HMS	Polyethylenimine	75	1	184	-	[74]
HMS	3-Aminopropyltrimethoxysilane	20	0.9	70	84	[75]
HMS	N-[3-(Trimethoxysilyl)propyl]-diethylenetriamine	20	0.9	53	42	[76]
As-syn HMS[a]	Dodecylamine	25	1	34	-	[74]
KIT-6	Tetraethylenepentamine	60	10	125	141	[77]
KIT-6	Polyethylenimine	75	1	135	-	[78]
Silica monolith	Polyethylenimine	75	1	210	260	[79]
Meso-structured monolith[a]	Tetraethylenepentamine	75	1	171	-	[80]
Mesocellular silica foam	Polyethylenimine	105	0.5	151	-	[81]
Mesocellular silica foam	Polyethylenimine	75	0.15	152	-	[82]
Mesocellular silica foam	Tetraethylenepentamine	75	0.1	201	-	[83]
Mesocellular silica	Polyethylenimine	45	0.1	55	-	[84]
As-syn silica mesocellular foam	Polyethylenimine	70	0.67	169	-	[85]
As-syn mesocelullar silica foam	Tetraethylenepentamine	75	1	198	229	[86]
MSU-H silica	3-[2-(2-Aminoethylamino)ethylamino] propyltrimethoxysilane	60	0.15	-	136	[87]
MSU-F	3-[2-(2-Aminoethylamino)ethylamino] propyltrimethoxysilane	45	0.3	72	-	[88]
MSU-F	Tetraethylenepentamine+ diethanolamine	50	1	260	-	[89]
Silica gel	3-Aminopropyltrimethoxysilane	27	1	18	41	[90]
Fumed silica	Polyethylenimine	25	0.0004	52	78	[91]
Fumed silica	3-[2-(2-Aminoethylamino) ethylamino]propyltrimethoxysilane	25	1	41	-	[92]
SiO_2 aerogel	3-Aminopropyltrimethoxysilane	25	0.1	86	307	[93]
Porous silica[a]	Tetraethylenepentamine	75	0.1	175	-	[94]
Macroporous silica	N-carboxyanhydride (NCA) of L-alanine	50	0.1	170	-	[95]
CARiACT G10 silica	Polyethylenimine	80	1	123	-	[96]
CARiACTVRG10	Polyethylenimine	80	1	166	-	[97]
Amine-bridged organosilica[a]	Bis((triethoxysilyl)propyl) ethylenediamine	0	1	101	-	[98]
R-IAS[b]	Secondary ethyleneamine	25	0.1	-	184	[99]
3N-APS-LAS-0.4[a]	3-Aminopropyltriethoxysilane	25	1	77	-	[100]
AF-MSM[a]	3-Aminopropyltriethoxysilane	60	0.2	24	-	[101]
Davisil™ (LC60A)	3-Aminopropyltriethoxysilane	25	1	62	94	[102]
Mesoporous silica capsules	Tetraethylenepentamine	75	0.1	-	349	[103]
Precipitated silica	N-[3-(Trimethoxysilyl)propyl] diethylenetriamine	40	1	45	-	[104]
G-silica sheets	Polyethylenimine	75	7	190	-	[105]
Double-walled silica nanotube	3-[2-(2-Aminoethylamino)ethylamino] propyl trimethoxysilane	25	1	98	-	[106]

[a]Amine-functionalized mesoporous silicas prepared by direct synthesis
[b]Reformulated immobilized amine sorbent

cept applied to just about all different classes of nanoporous materials for CO_2 capture over the last decade. This article reviews the recent advances in amine-functionalized nanoporous materials as CO_2 adsorbents with particular emphasis on their preparation methods and CO_2 capture performance based on their equilibrium CO_2 uptake.

AMINE-FUNCTIONALIZED MESOPOROUS SILICA

Mesoporous silica materials are normally prepared using different types of surfactant molecules as a soft template using a silicate precursor in an aqueous medium. Extensive reviews on the synthesis and classification of mesoporous silica materials are available elsewhere [40-42]. Mesoporous silica has outstanding textural and surface properties, such as large surface area, large pore volume, adjustable mesopore size, and abundant surface hydroxyl groups available for diverse post-synthesis functionalization. These features make mesoporous silica a primary candidate support material for amine guest molecules to produce hybrid materials for capturing CO_2. Table 1 lists the CO_2 capture works reported using amine-functionalized mesoporous silica adsorbents.

1. Amine-impregnated Mesoporous Silica

In amine-functionalized mesoporous silica prepared by physical impregnation methods, a large quantity of amine species, approximately 40 to 70 wt%, can be accommodated inside the channels of the silica support (Fig. 4). Typically, amine species are dissolved in a polar solvent (methanol or ethanol) and mixed with calcined mesoporous silica powders. The resulting slurry is stirred continuously and a mild vacuum is applied to promote the transport of amine species to the pore interiors before being finally dried at a specific temperature to remove the solvent [43]. To achieve a fine distribution of amines inside the pores, it is important to estimate the total pore volume of the support material before amine impregnation, so a correct amount of amine that matches the pore volume of the support can be introduced.

As shown in Table 1, different types of mesoporous silica materials have been tested as a support for amine impregnation. Xu et al. [43-45] first reported an amine-impregnated mesoporous silica for CO_2 capture. Their PEI (polyethylenimine)-impregnated MCM-41 showed high CO_2 capture capacity (110-133 mg/g $_{adsorbent}$, 75 °C, 1 atm) [43] and excellent capture selectivity [44]. The adsorbent can be regenerated at 75 °C, and moisture was found to have a complementary effect on the adsorption of CO_2 by promoting the formation of hydrogen carbonate [45]. In addition, the PEI-impregnated MCM-41 was stable in the cyclic operations of CO_2 adsorption separation from moist flue gas. These encouraging results triggered subsequent studies on amine-impregnated mesoporous silica for CO_2 capture. Franchi et al. [50] impregnated DEA (diethanolamine) onto a pore-expanded MCM-41, which could accommodate a large quantity of amine (7.26 mmol DEA/g $_{adsorbent}$) and achieve a maximum capacity of 104 g CO_2/g $_{adsorbent}$ (25 °C, 0.05 atm). The hybrid material quickly desorbed all the captured CO_2 by heating at 75 °C in N_2. At CO_2 partial pressures below 0.15 atm, the hybrid adsorbent was found to be superior to zeolite 13X, especially under conditions with moisture. Repeated adsorption/desorption cycles revealed its good cyclic stability. Similarly, Subagyono et al. [81] reported a PEI-impregnated mesocellular siliceous foam (MCF) for CO_2 capture that had a large pore volume (2.5 cm^3/g) and pore size (31 nm). The adsorption capacity of MCF loaded with PEI reached 151 mg/g $_{adsorbent}$ in 20 min adsorption time (105 °C, 0.5 atm), which was improved significantly over the adsorption capacity observed for SBA-15 loaded with PEI (107 mg/g $_{adsorbent}$) under the same conditions. Son et al. [78] impregnated PEI onto different types of mesoporous silica support materials and compared their performance for CO_2 capture. The CO_2 adsorption capacities of the materials decreased according to the following sequence: KIT-6>SBA-16≈SBA-15>MCM-48>MCM-41, as dictated by the mean pore diameter of the support material. The pore diameter of the support material was also found to be the most important variable with respect to controlling the adsorption kinetics, provided that all of the amine species could be accommodated inside the pores. The PEI-impregnated KIT-6 also exhibited stable adsorption-desorption in three consecutive test cycles (adsorption and desorption at 75 °C) for 900 min.

Chen et al. [74] reported the importance of textural mesoporosity (interparticle pores) in HMS mesoporous silica supports for CO_2 capture, which can lead to an increase in the concentration of amine species inside the pore structure and facilitate CO_2 diffusion inside the pore channels. They then proposed an improved CO_2 adsorbent by impregnating PEI onto a silica monolith with a hierarchical meso-macroporous structure and large pore volume and textural mesoporosity, which exhibited a CO_2 adsorption capacity of 210 mg CO_2/g $_{adsorbent}$ (75 °C, 1 atm) at a 65 wt% PEI loading [79]. Reversible and stable CO_2 adsorption-desorption performance during five repeated runs (adsorption and desorption at 75 °C) was observed.

Yue et al. developed a highly efficient CO_2 adsorbent by impregnating TEPA (tetraethylenepentamine) onto an as-synthesized meso-

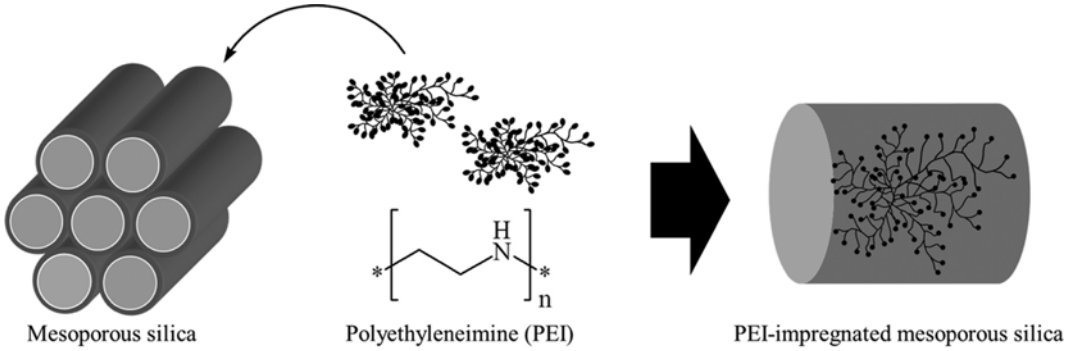

Fig. 4. Preparation of amine-functionalized mesoporous silica using a physical impregnation method [43].

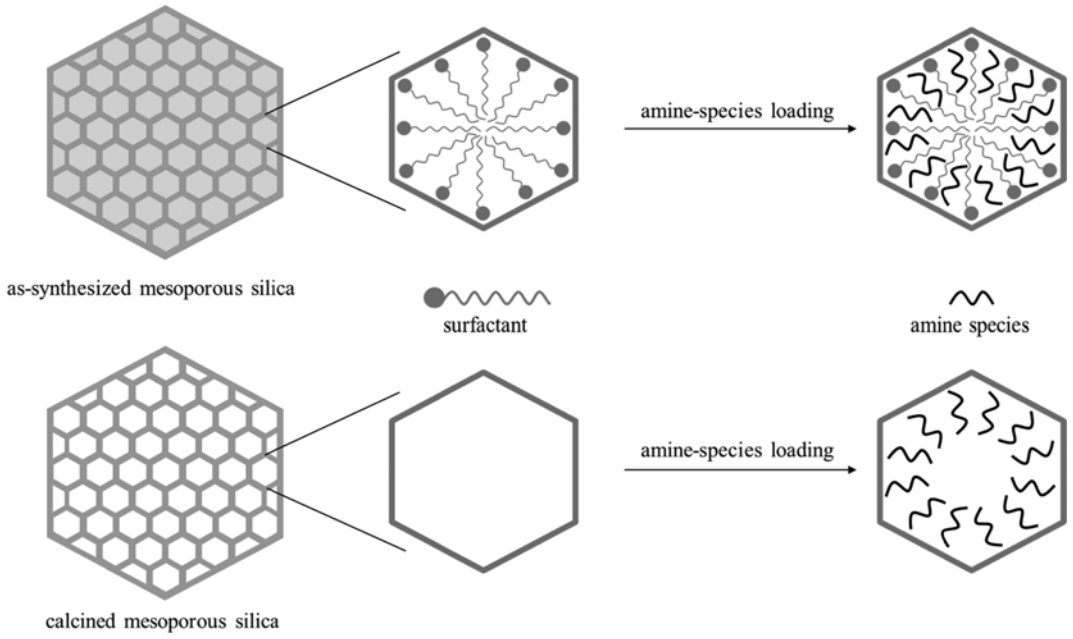

Fig. 5. Schematic diagram depicting the influence of the template occluded in a channel of MCM-41 on the distribution of amine species [54].

porous silica-MCM-41 and SBA-15 [54,70]. Instead of removing the surfactant by calcination to form mesopores for subsequent amine immobilization, they impregnated amine directly onto the as-synthesized mesoporous silica (Fig. 5). The ionic surfactant CTAB (hexadecyltrimethylammoniumbromide) molecules were dispersed in the channels of MCM-41, like the spokes in a wheel. The amine guest could be distributed in the micelles of the support, forming a web within the mesopores to trap CO_2 molecules. The material exhibited a high adsorption capacity at low CO_2 concentrations; the value achieved in 5% CO_2 at 75 °C (200 mg/g) was close to that in pure CO_2 (211 mg/g), and the adsorption capacity in the sixth recycle showed only ca. 8.5% capacity loss. It was claimed to be competitive due to the energy and time savings made in the preparation of the support material (no need to remove the surfactant) along with the high CO_2 adsorption capacity.

Yang et al. [105] reported a sandwich-like, high-surface-area, graphene-based mesoporous silica (G-silica) sheet as a support for PEI impregnation. The resulting PEI/G-silica sheet was claimed not only to possess high loading content of PEI, but also exhibit high thermal conductivity owing to the presence of graphene, which can efficiently prevent overheating in adsorbent matrix and avoid degradation of PEI. PEI/G-silica sheets exhibited a stable adsorption/desorption cycle performance (adsorption at 75 °C and desorption at 120 °C) with a high adsorption capacity of 171 mg/g at 1 atm. As shown in Table 1, PEI and TEPA are the two most widely investigated amine species to prepare amine-impregnated mesoporous silica for CO_2 capture, possibly due to their high N atom concentration (PEI and TEPA have N contents of 33% and 37%, respectively). A high CO_2 uptake was normally achieved at relatively high temperatures (e.g., 75 °C) by PEI or TEPA-impregnated mesoporous silica, due to the improved mobility of amine species and facilitated the diffusivity of CO_2 within it at relatively high temperatures [81]. On the other hand, the thermal stability of amine-impregnated silica can be problematic because there is no chemical bonding formed between the amine species and support. For example, a decrease in CO_2 capacity was observed after repeated runs for TEPA-impregnated mesoporous silica due to the leaching of the physisorbed TEPA from the support [67,79].

2. Amine-grafted Mesoporous Silica

As shown in Table 1, a range of mesoporous silica, such as MCM-41, SBA-15, SBA-16, SBA-12, MSU, HMS and MCM-48, has been investigated as a support material for amine grafting, whereas aminosilanes of monoamine (3-aminopropyl-triethoxysilane), diamine ([N-(2-aminoethyl)-3-aminopropyl]trimethoxysilane), and triamine (3-[2-(2-aminoethylamino) ethylamino]propyltrimethoxysilane) have been employed mostly as grafting agents (see Fig. 3 for their chemical structures). Amine groups are mostly introduced to the mesoporous silica structures through a condensation reaction between aminosilanes and hydroxyl groups on the mesoporous silica surface (Fig. 6). In a typical preparation of amine-grafted mesoporous silica, pretreated nanoporous support powders were dispersed in the solvent (e.g. toluene) with stirring, and the desired quantity of amine was then added and kept in solution under reflux. A higher concentration of hydroxyl groups on the mesoporous silica surface is favorable for achieving a high amine species loading.

Huang et al. [55] examined CO_2 capture by an amine-grafted silica xerogel and MCM-48 using 3-aminopropyltriethoxysilane as a grafting agent. A CO_2 uptake of 27 mg/g $_{adsorbent}$ and 50 mg/g $_{adsorbent}$ was achieved by amine-surface-modified silica xerogel and MCM-48 (25 °C, 0.05 atm), respectively. It was found that the presence of water vapor doubled the amount of CO_2 adsorbed. Chang et al. [65] examined the adsorption of CO_2 on amine-grafted mesoporous silica. MCM-41, SBA-15 and pore-expanded MCM-41 were modified by mono-, di- and tri-aminosilanes to make hybrid adsorbents for CO_2 capture. SBA-15 was found to be a better support than MCM-41 or pore-expanded SBA-15 for grafting amine moieties for the adsorption of CO_2. The tri-amine-grafted SBA-15 exhibited a CO_2 adsorption capacity as high as 106 mg/g $_{adsorbent}$ under anhydrous gas

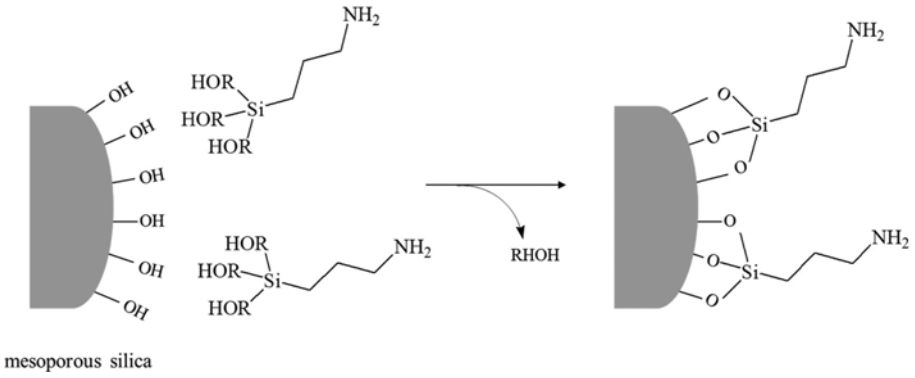

Fig. 6. Preparation of amine-functionalized mesoporous silica through a chemical grafting method (R represents CH_2- or CH_2CH_2-) [52].

flow and 120 mg/g $_{adsorbent}$ under humid gas flow conditions (60 °C, 0.15 atm). Harlick et al. [52] grafted triamine onto the surface of pore-expanded MCM-41 to produce a hybrid CO_2 adsorbent. A high amine content was achieved using pre-hydrated silica surfaces at grafting temperatures under reflux conditions, which can facilitate thermally controlled water-aided surface polymerization of the aminosilanes (Fig. 7). The triamine-grafted pore-expanded MCM-41 achieved a CO_2 capture capacity of 117 mg/g $_{adsorbent}$ and 129 mg/g $_{adsorbent}$ under dry and humid (25 °C, 0.05 atm) conditions, respectively. The triamine-grafted pore-expanded MCM-41 outperformed commercial zeolite 13X. Owing to the higher amine content, triamine-grafted mesoporous silica often results in a high CO_2 uptake. On the other hand, the large pore size in the mesoporous silica support is necessary to facilitate the diffusion of CO_2 inside the pore channels to contact with bulky CO_2-affinity sites.

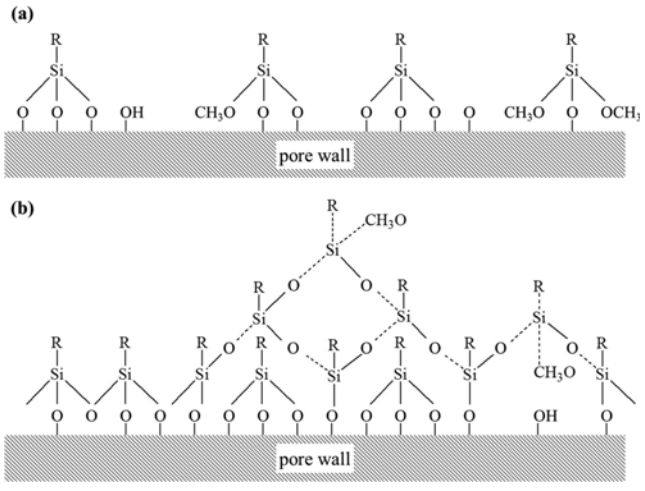

Fig. 7. (a) Proposed surface structure obtained with anhydrous grafting; (b) proposed early stage growth of a 3-D polyaminosiloxane layer that occurs during the grafting of alkoxy-silane compounds in the presence of water. The R group represents a triamine chain, and the dashed lines represent the out of plane orientation of the bold groups [52].

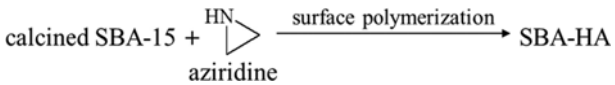

Fig. 8. Hyperbranched amino silica prepared by a one-step reaction between aziridine and silica surface [67].

Rather than using aminosilanes as the amine source for grafting, Choi et al. [66] and Hicks et al. [67] prepared hyperbranched aminosilica using aziridine as a grafting agent. The surface silanols of mesoporous silica, SBA-15, initiated aziridine polymerization off the surface (Fig. 8). At room temperature under humid conditions, the CO_2 uptake of the hyperbranched aminosilica varied from 166 to 76 mg/g $_{adsorbent}$ when the CO_2 concentration was changed from 10% to 400 ppm. Similarly, Liu et al. [95] synthesized a covalently tethered CO_2 adsorbent through the in situ polymerization of N-carboxyanhydride (NCA) of L-alanine on the amine-functionalized three-dimensional interconnected macroporous silica. The adsorbent exhibited an adsorption capacity of up to 170 mg CO_2/g $_{adsorbent}$ under simulated flue gas conditions (50 °C, 0.1 atm).

3. Amine-functionalized Mesoporous Silica Prepared by Direct Synthesis

Instead of incorporating amine groups into mesoporous silica through a post synthesis method, amine-functionalized mesoporous silica can also be prepared using direct methods. Tang et al. [98] synthesized amine-bridged organosilica by hydrolysis and the polycondensation of bis((triethoxysilyl)propyl) ethylenediamine and tetraethoxysilane in the presence of an anionic surfactant as a structure-directing agent. This organosilica showed high CO_2 sorption capacities up to 101 mg/g $_{adsorbent}$ (0 °C, 1 atm). Kim et al. [100] prepared amine-functionalized mesoporous silica using the anionic surfactant-mediated synthesis method reported by Che et al. [107], in which 3-aminopropyltriethoxysilane functions as a silica source and as a co-structure directing agent (Fig. 9). The highest CO_2 capture capacity achieved was ca. 77 mg/g $_{adsorbent}$ (25 °C, 1 atm). Covalently bonded amine species in the mesoporous silica were robust enough to maintain steady adsorption performance during ten repetitions of the adsorption-desorption cycle (desorption at 75 °C). Wen et al. [80] synthesized an amine-functionalized mesostructured silica monolith in a one-pot process, where TEPA was used not only as the modifier coating onto the resulting monolith, but also as an the additive controlling the generation of micropores in the silica wall. The resulting TEPA containing monoliths possessed considerable mechanistic strength, and exhibited CO_2 adsorption capacity up to 171 mg/g $_{adsorbent}$ (75 °C, 1 atm).

Generally, larger number of amine groups can be loaded onto a mesoporous silica support by physical impregnation. Amine-impreg-

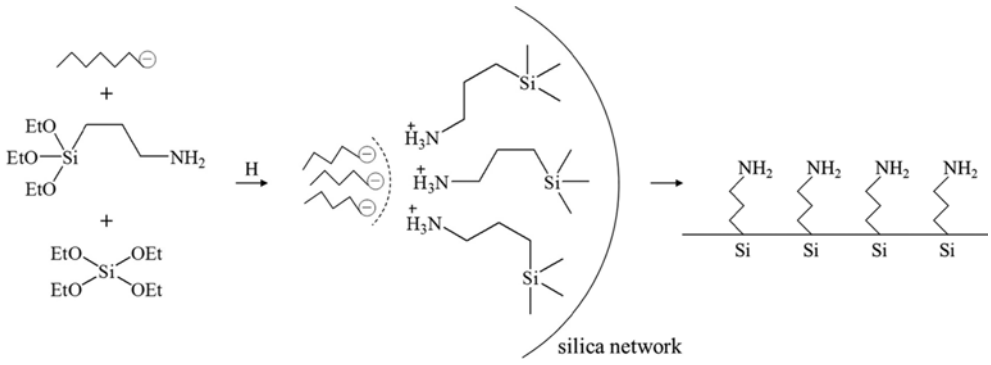

Fig. 9. Preparation of amine-functionalized mesoporous silica using a direct synthetic method [100].

nated mesoporous silica, however, can suffer from the leaching of amine species from the support material at relatively high temperatures because no chemical bonding between the amine species and matrix is achieved [67,79]. Introducing amine groups to mesoporous silica through chemical grafting or direct synthesis can result in a more stable CO_2 adsorbent. On the other hand, the number of amine guests introduced in the latter is limited by the population of silanol groups on the mesoporous silica surface, which normally leads to lower CO_2 uptake compared to those achieved by amine-impregnated mesoporous silica.

AMINE-FUNCTIONALIZED MESOPOROUS ALUMINA

Mesoporous alumina also exhibits high surface area, narrow pore size distribution in the mesopore region, and large pore volume. The intrinsic basicity in the material can also be exploited for CO_2 capture. Despite this, few groups have investigated mesoporous alumina as a support material for amine species to produce hybrid materials for CO_2 capture. Amine-functionalized mesoporous alumina has been prepared only through physical impregnation methods.

Chen et al. [108] impregnated PEI onto mesoporous alumina. The amine-impregnated mesoporous alumina exhibited a CO_2 capture capacity of 120 mg/g $_{adsorbent}$ (75 °C, 1 atm), which is comparable to that achieved by PEI impregnated MCM-41 reported by Xu et al. [44]. This PEI-impregnated mesoporous alumina exhibited stable adsorption-desorption during five consecutive test cycles (adsorption and desorption at 75 °C). Chaikittisilp et al. [109] prepared mesoporous γ-alumina-supported PEI composite materials using a physical impregnation method. The PEI-alumina adsorbents outperformed the silica-supported counterparts in terms of their capture capacity and amine efficiency, particularly at low CO_2 concentrations in ambient air conditions. Plaza et al. [110] immobilized amines on an alumina support through a wet impregnation method. The sample impregnated with diethylenetriamine showed a CO_2 uptake of ca. 80 mg/g $_{adsorbent}$ (100 °C, 1 atm), whereas the raw alumina achieved ca. 10 mg/g $_{adsorbent}$ under the same conditions.

AMINE-FUNCTIONALIZED ZEOLITES AND CARBONS

Microporous materials, such as zeolite and carbon, have been investigated for CO_2 capture through physisorption under low temperature conditions. Owing to their relatively small surface area and pore volume compared to mesoporous materials, post-synthesis amine-functionalization has been attempted to achieve enhanced CO_2 selectivity over N_2, often at the expense of reduced CO_2 capture capacity. Table 2 gives a summary of the reported performance data involving amine-functionalized zeolites and carbon for CO_2 capture.

1. Amine-functionalized Zeolites

Jadhav et al. [111] impregnated MEA on zeolite 13X and examined the hybrid material for CO_2 adsorption at different temperatures. The MEA-impregnated adsorbent showed higher CO_2 capture capacity than zeolite 13X at 120 °C, and exhibited improved CO_2 selectivity, which was enhanced further in the presence of moisture. Su et al. [113] modified a commercially available Y-type zeolite by TEPA using a physical impregnation method. The CO_2 adsorption capacity of the adsorbent increased with increasing temperature at 30-60 °C but decreased between 60-70 °C. The CO_2 adsorption capacity was affected by water vapor and reached as much as 113 mg/g of CO_2/g $_{adsorbent}$ (60 °C, 0.15 atm) at 7% water vapor. The adsorption capacity was preserved after 20 cycles of adsorption and regeneration at 75 °C. Xu et al. [114] examined the adsorptive separation of CO_2, CH_4 and N_2 on MEA-modified β-zeolite prepared using a physical impregnation method, and found that the incorporation of MEA improved the selectivity of both CO_2/CH_4 and CO_2/N_2.

Amine-functionalized zeolites prepared through chemical grafting have been investigated for CO_2 capture. Kim et al. [115] examined the CO_2 separation from N_2 over 3-aminopropyltrimethoxysilane-grafted mesoporous SAPO-34, which had been synthesized using an amphiphilic organosilane additive. Despite the decrease in CO_2 capture capacity due to the reduced surface area and pore volume, the amine-grafted mesoporous SAPO-34 showed significantly improved CO_2/N_2 selectivity via the preferential adsorption of CO_2 over N_2. Approximately 96% of the adsorbed CO_2 could be desorbed reversibly by simply changing of the feed gas to a N_2 purge during the five adsorption-desorption cycles. Yang et al. [116] studied CO_2 capture over amine-grafted MCM-22, MCM-36 and ITQ-2. They reported that amine-grafting on zeolites in general resulted in an enhancement of CO_2/N_2 selectivity and increased heat of CO_2 adsorption at the expense of reduced CO_2 capture capacity. More than 95% desorption was achieved by heating at 75 °C and their regeneration was very reproducible. Zukal et al. [117] grafted amine onto a delaminated zeolite ITQ-6, which possesses a large hydroxylated and accessible external surface. They reported that the adsorp-

Table 2. CO_2 capture by amine-functionalized mesoporous alumina, zeolite, carbon, porous polymer, and other nanoporous materials

Support materials	Amine type	Temp. (°C)	CO_2 partial pressure (atm)	CO_2 adsorption capacity (mg/g)		Reference
				Dry CO_2	Humid CO_2	
Mesoporous alumina	Polyethylenimine	75	1	120	-	[108]
Mesoporous γ-alumina	Polyethyleneimine	25	0.0004	77	-	[109]
Commercial activated alumina	Diethylenetriamine	100	1	80	-	[110]
Zeolite 13 X	Monoethanolamine	75	0.15	36	30	[111]
Zeolite 13X	Isopropanolamine	75	0.15	23	-	[112]
Y-type zeolite	Tetraethylene pentamine	60	0.15	113	190	[113]
β-Zeolite	Monoethanolamine	30	1	61	-	[114]
Mesoporous SAPO-34	3-Aminopropyl trimethoxysilane	0	1	121	-	[115]
Zeolite ITQ-2	3-Aminopropyl trimethoxysilane	0	1	94	-	[116]
Zeolite ITQ-6	3-Aminopropyl trimethoxysilane	20	1	53	-	[117]
Carboxylate-rich carbonaceous materials	Tris(2-aminoethyl) amine	−20	1	189	-	[118]
Multi-wall carbon nanotube	3-Aminopropyl trimethoxysilane	50	0.15	86	108	[119]
Multi-wall carbon nanotube	3-Aminopropyl triethoxysilane	20	0.15	55	-	[120]
Single-wall carbon nanotube	Polyethylenimine	75	1	78	-	[121]
Activated fly ash derived sorbent	Monoethanolamine	30	1	68.6	-	[122]
Fly ash carbon concentrate	3-Chloropropylamine hydrochloride	25	0.1	-	8	[123]
Commercial activated carbon	Polyethylenimine	25	1	49	-	[124]
Porous polymer	Melamine	25	1	59	-	[125]
Porous organic polymer	Ethylenediamine	25	1	42	-	[126]
Nanofibrillated cellulose	N-(2-Aminoethyl)-3-aminopropyl methyldimethoxysilane	25	0.0005	-	61	[127]
Mesoporous TiO_2 bead	L-Arginine	30	0.2	18	-	[128]
Bentonite	Polyethylenimine	75	1	47	-	[129]

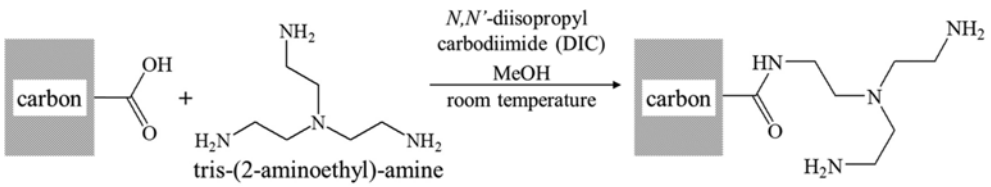

Fig. 10. Preparation of amine-rich materials through grafting of carbon spheres derived from hydrothermal synthesis [118].

tion of CO_2 occurs simultaneously on both amine ligands and bare surface. At low CO_2 pressures, ammonium carbamates were formed, but adsorption on the bare surface appeared to dominate under higher pressures.

2. Amine-functionalized Carbon

Zhao et al. [118] reported carbonaceous materials with a high surface density of amino groups for CO_2 adsorption. They prepared carboxylate-rich carbonaceous materials by the hydrothermal carbonization of glucose in the presence of small amounts of acrylic acid. The carboxylic acid groups of hydrothermally derived carbon microspheres with a raspberry-like substructure were then used to anchor tris(2-aminoethyl)amine via amide formation through condensation reactions (Fig. 10). The amine-grafted carbonaceous material showed a CO_2 uptake of 189 mg/g $_{adsorbent}$ (−20 °C, 1 atm) and exhibited a CO_2 selectivity of 110 against N_2 at 70 °C, 1 atm. Dillon et al. [121] achieved carbon dioxide adsorption through the covalent attachment of polyethyleneimine-functionalized single-wall carbon nanotubes. The reaction between fluorinated single-wall carbon nanotubes (F-SWNTs) and polyethyleneimine (PEI) yielded the covalent attachment of a polymer to the sidewalls of the nanotubes (Fig. 11). Solid-state ^{13}C NMR confirmed carbamate formation as a consequence of the reversible CO_2 absorption to the primary amine substituents in PEI. A maximum absorption of 78 mg/g $_{adsorbent}$ was observed (75 °C, 1 atm) and desorption of CO_2 was accomplished by heating under argon at 75 °C. Gray et al. [123] reported CO_2 capture by amine-enriched fly ash carbon adsorbents. The amine groups

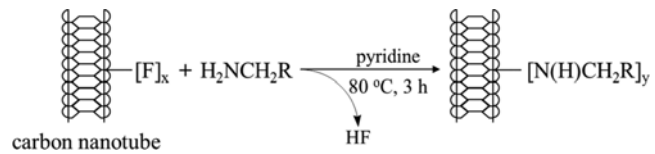

Fig. 11. Synthesis of functionalized SWNTs from F-SWNTs [121].

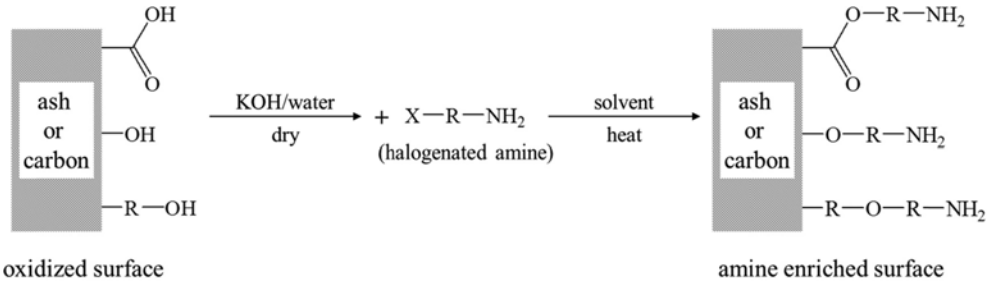

Fig. 12. Proposed reactions for the preparation of amine-enriched fly ash or carbon sorbent [123].

were grafted by a chemical treatment of carbon-enriched fly ash concentrates with a 3-chloropropylamine-hydrochloride solution at 25 °C (Fig. 12). These materials, however, achieved very low CO_2 capture capacity (8 mg/g $_{adsorbent}$ at 25 °C, 0.1 atm).

Generally, as a support material for amine species to produce hybrid adsorbents for CO_2 capture, zeolite and carbon are not comparable to mesoporous silica due to their smaller pore volumes and pore sizes. Unlike mesoporous silica materials, which exhibit practically negligible CO_2 capture capacities, zeolite and microporous carbon are normally capable of capturing significant amounts of CO_2 through physisorption. The incorporation of amine species would certainly reduce the surface area and pore volume of a zeolite or carbon, and cause the loss of CO_2 capture capacity. In some cases, the CO_2 capture capacity from the introduced amine species does not compensate for the lost CO_2 capture capacity by physisorption because of the decrease in active surface area. On the other hand, amine introduced in zeolites or carbon alter the adsorption mechanism from physical adsorption to chemisorption or combined physi-chemisorption mechanism (depending on the amine loading), and the capture selectivity towards CO_2 is enhanced, which can be improved further in the presence of moisture or at relatively higher temperatures.

AMINE-FUNCTIONALIZED POROUS POLYMER

Some studies have reported CO_2 capture by amine-functionalized porous polymers. Chen et al. [125] prepared an amine-containing porous polymer by the condensation of melamine with several aromatic aldehydes through Schiff base chemistry (Fig. 13) according to the protocol developed by Schwab et al. [130]. This melamine-based porous polymer exhibited a CO_2 capture capacity of 59 mg/g $_{adsorbent}$ (25 °C, 1 atm), which was attributed mostly to the amine groups inside the porous framework and were comparable to some reported values of amine-grafted nanoporous silica. Gebald et al. [127] synthesized an amine-functionalized nanoporous material by freeze-drying an aqueous suspension of nanofibrillated cellulose and N-(2-aminoethyl)-3-aminopropylmethyldimethoxysilane. The resulting materials achieved a CO_2 capture capacity of 61 mg/g $_{adsorbent}$ in 12 h at a CO_2 concentration of 506 ppm in air and a relative humidity of 40% at 25 °C. Stability over 20 consecutive 2-h-adsorption/1-h-desorption cycles (adsorption at a CO_2 concentration of 506 ppm in air and a relative humidity of 40% at 25 °C and desorption in Ar at 90 °C and 40% relative humidity) was examined, which yielded a cyclic capture capacity of 31 mg CO_2/g $_{adsorbent}$. Guillerm et al. [126] synthesized a porous organic polymer with free aldehyde moieties, which allowed a deliberate amine grafting (aldehyde conversion to imine) via a mild one-step post-synthetic modification procedure. Amine-functionalization led to ca. 20% increase in CO_2 capture capacity, a substantial increase in Q_{st} (i.e., from 33 to 50 kJ/mol at low coverage), and a relatively enhanced qualitative CO_2/N_2 and CO_2/CH_4 selectivity (14 to 155 for CO_2/N_2 and 5 to 600 for CO_2/CH_4).

AMINE-FUNCTIONALIZED POROUS TiO_2

Aquino et al. [128] reported amine-functionalized TiO_2-based

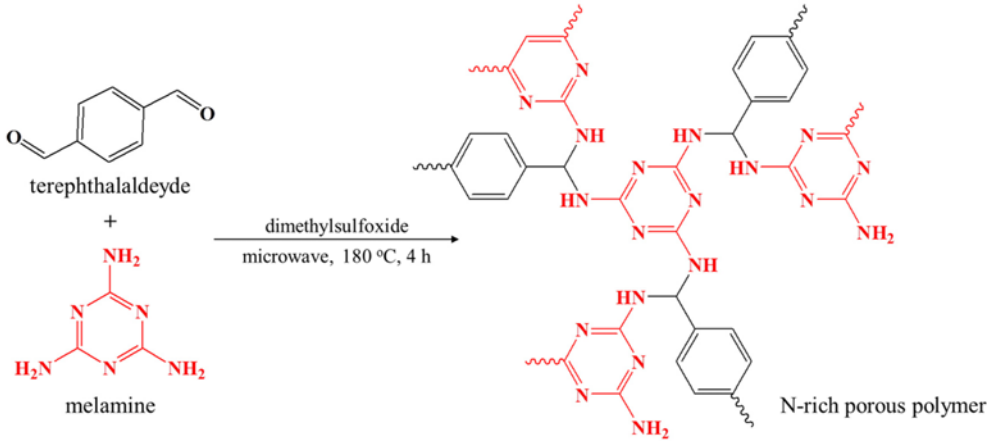

Fig. 13. Preparation of amine-containing porous polymer through Schiff-base chemistry [130].

sorbents for CO_2 capture. Several supports, namely, mesoporous TiO_2 beads, TiO_2 nanoparticles, and TiO_2/ZrO_2 composite beads, and a range of amines (1, 2, and 3 carbon-chain primary amine) have been assessed for CO_2 adsorption. The highest CO_2 adsorption capacity (18 mg CO_2/g $_{adsorbent}$ at 30 °C and 20 kPa CO_2) was achieved by L-arginine functionalized mesoporous TiO_2 bead.

AMINE-FUNCTIONALIZED CLAY

Chen et al. [129] reported surface modification of a low cost bentonite through PEI impregnation for CO_2 capture. The CO_2 uptake and capture selectivity over N_2 increased significantly after amine modification, and the PEI-modified bentonite exhibited excellent stability in cyclic CO_2 adsorption-desorption runs (adsorption and desorption at 75 °C). PEI-modified bentonite was claimed to be a potential adsorbent for practical application in post-combustion CO_2 capture, owing to its CO_2 capture performance, easy preparation, and low cost of bentonite.

AMINE-FUNCTIONALIZED MOFs

MOFs have attracted considerable attention for their potential applications in CO_2 capture and separation, due mainly to their well-ordered porous structures that exhibit extremely high inner surface areas, high pore volumes and tunable chemical functionality provided by their organic moieties. Over the last decade, the functionalization of MOFs with amine groups has been reported to be an efficient strategy for enhancing the CO_2 capture performance of these materials. Table 3 provides a summary of the reported performance data involving amine-functionalized MOFs for CO_2 capture.

1. Amine-functionalized MOFs Prepared by Direct Synthesis

A number of amine-functionalized MOFs have been prepared directly using amine-containing ligands as organic linkers to form crystalline MOF structures. Several groups have reported amine-functionalized MOFs synthesized using 2-aminoterephthalic acid as the organic ligand. Lin et al. [131] synthesized amine-functionalized MIL-101(Cr) using an OH^--assisted hydrothermal technique

Table 3. CO_2 capture by amine-functionalized MOFs

Adsorbent	Amine type	Temp. (°C)	CO_2 partial pressure (atm)	Dry CO_2 adsorption capacity (mg/g)	Reference
NH_2-MIL-101(Cr)	2-Amino-1,4-benzenedicarboxylic acid	16	25	660	[131]
TEPA-MIL-101(Cr)	Tetraethylenepentamine	25	1	124	[132]
DETA-MIL-101(Cr)	Diethylenetriamine	0	1	79	[133]
NH_2-MIL-101(Al)	2-Amino-1,4-benzenedicarboxylic acid	25	30	616	[134]
NH_2-MIL-53(Al)	2-Amino-1,4-benzenedicarboxylic acid	30	30	295	[135]
NH_2-MIL-53(Al)	2-Amino-1,4-benzenedicarboxylic acid	10	28	334	[136]
NH_2-MIL-53 (Al)	2-Amino-1,4-benzenedicarboxylic acid	25	1	80	[137]
NH_2-Zr-MOF	2-Amino-1,4-benzenedicarboxylic acid	0	1	196	[138]
CAU-1	2-Amino-1,4-benzenedicarboxylic acid	0	1	317	[139]
USO-2-Ni-A	2-Amino-1,4-benzenedicarboxylic acid	25	1	140	[140]
$(Me_2NH_2)In(NH_2BDC)_2$	2-Amino-1,4-benzenedicarboxylic acid	25	30	339	[141]
ED-Mg/DOBDC	Ethylenediamine	25	0.0004	66	[142]
ZTF-1	5-Aminotetrazole	0	1	246	[143]
Mmen-Mg_2(dobpdc)	*N,N'*-Dimethylethylenediamine	25	0.0004	88	[144]
$Cu_{24}(TPBTM^{6-})_8(H_2O)_{24}$	*N,N',N''*-Tris(isophthalyl)-1,3,5-enzenetricarboxamide	25	20	1034	[145]
$Cu_3(btc)_2$(3-picolylamine)$_2$	3-Picolylamine	0	1	140	[146]
UMCM-1-NH_2	2-Amino-1,4-benzenedicarboxylic acid	0	1	64	[147]
UMCM-1-NH_2	2-Amino-1,4-benzenedicarboxylic acid	25	18	869	[148]
NJU-Bai3	5-(4-Carboxybenzoylamino)-isophthalic acid	0	1	273	[149]
CPF-13	3,5-Diamino-1,2,4-triazole	25	1	159	[150]
Mmen-CuBTTri	*N,N'*-Dimethylethylenediamine	25	0.15	105	[151]
$H_3[(Cu_4Cl)_3(BTTri)_8]$-en	Ethylenediamine	25	1	55	[152]
$Zn_2(C_2O_4)(C_2N_4H_3)_2(H_2O)_{0.5}$	3-Amino-1,2,4-triazole	0	1.2	191	[153]
bio-MOF-11	Adenine	0	1	264	[154]
$Zn_2(Atz)_2$(ox)	3-Amino-1,2,4-triazole	0	1	189	[155]
PPN-6-CH_2DETA	Diethylenetriamine	22	1	189	[156]
$[Cd(NH_2\text{-bdc})(bphz)_{0.5}]\cdot DMF\cdot H_2O\}_n$	2-Aminobenzenedicarboxylic acid+ 1,2-bis(4-pyridylmethylene) hydrazine	−78	1	230	[157]
ZIF-en	Ethylenediamine	35	10	211*	[158]

* mg CO_2/cm^3 $_{adsorbent}$

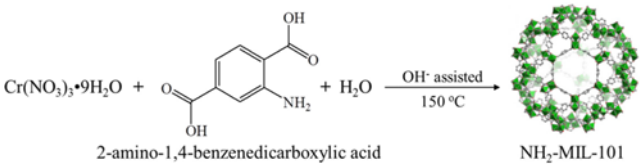

Fig. 14. Synthesis of amine-functionalized MIL-101(Cr) using an OH-assisted hydrothermal technique [131].

(Fig. 14). The prepared MOF possessed a surface area up to 1,675 m^2/g, small mean particle size of approximately 50 nm, and a CO_2 capture capacity of up to 660 mg/g $_{adsorbent}$ (16 °C, 25 atm). Si et al. [139] reported amine-decorated 12-connected MOF CAU-1 synthesized using 2-aminoterephthalic acid as organic ligand that exhibited a high heat of adsorption for CO_2 (48 kJ/mol), high CO_2 uptake capacity (317 mg/g $_{adsorbent}$ at 0 °C, 1 atm), and an impressive selectivity for CO_2 over N_2 (101 : 1 at 0 °C). Arstad et al. [140] synthesized three types of amine-functionalized MOFs based on Al, Ni and In. At 25 °C, the highest CO_2 adsorption capacities achieved by these amino-functionalized adsorbents reached 140 mg/g $_{adsorbent}$ at a CO_2 pressure of 1.0 atm.

Some also reported the direct synthesis of amine-functionalized MOFs using amine-containing azole as an organic linker. Panda et al. [143] reported a three-dimensional amine-functionalized zeolitic tetrazolate framework (ZTF-1) produced from a reaction of $Zn(NO_3)_2$ with 5-aminotetrazole in a *N,N*-dimethylformamide (DMF) solution in the presence of *N,N*-dimethylformamide-azine-dihydrochloride (Fig. 15), which showed a CO_2 uptake of 246 mg/g $_{adsorbent}$ (0 °C, 1 atm). Zhai et al. [150] reported an anionic porous framework with amine-decorated polyhedral cages using 3,5-diamino-1,2,4-triazole and 1,4-H_2BDC as complementary ligands, which exhibited a CO_2 uptake capacity of 159 mg/g $_{adsorbent}$ (25 °C, 1 atm), as well as high CO_2/N_2 and CO_2/CH_4 selectivity (31 : 1 for $CO_2 : N_2$, and 5 : 1 for $CO_2 : CH_4$ at 0 °C, 1 atm). Vaidhyanathan et al. [153] reported an MOF with amine-lined pores. The material was synthesized solvothermally using zinc carbonate with 3-amino-1,2,4-triazole and oxalic acid as the organic ligand and co-ligand, respectively; a CO_2 uptake of 191 mg/g $_{adsorbent}$ (0 °C, 1.2 atm) was obtained.

Zheng et al. [145] reported an *rht*-type MOF constructed from a hexacarboxylate ligand with acylamide groups, *N,N',N''*-tris(isophthalyl)-1,3,5-benzenetricarboxamide. This compound exhibited a large CO_2 uptake of 1,034 mg/g $_{adsorbent}$ (25 °C, 20 atm), enhanced heat of adsorption, and higher selectivity toward CO_2/N_2 compared to an analogous MOF with alkyne groups, PCN-61. Duan et al. [149] reported an *agw*-type porous framework (NJU-Bai3) with inserted amide functional groups, based on 5-(4-carboxybenzoylamino)-isophthalic acid as a multidentate ligand. This compound exhibited

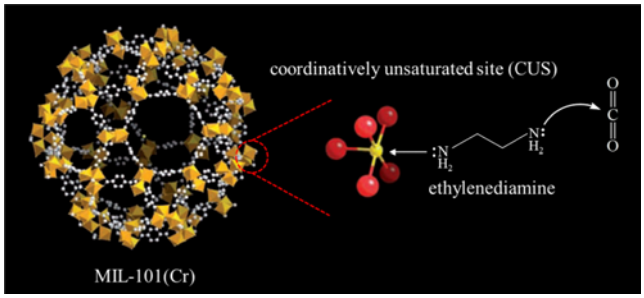

Fig. 16. Surface functionalization of the dehydrated MIL-101 through selective grafting of amine molecules (i.e. ethylenediamine) onto coordinatively unsaturated sites, and followed by the attack of an amino group on CO_2 [133].

a CO_2 storage capacity of 273 mg/g $_{adsorbent}$ (0 °C, 1 atm), high adsorption heat (36.5 kJ/mol), and highly selective CO_2 capture over N_2 and CH_4 (60.8 for CO_2: N_2 and 46.6 for CO_2: CH_4 at 0 °C, 20 atm). An et al. [154] synthesized cobalt adeninate bio-MOFs using adenine as a building block for CO_2 capture. The bio-MOF-11 had a CO_2 capacity of 264 mg/g $_{adsorbent}$ (0 °C, 1 atm), high heat of adsorption for CO_2 (45 kJ/mol), and impressive selectivity for CO_2 over N_2 (81 : 1 at 0 °C). Haldar et al. [157] reported two isomeric MOFs composed of a mixed-ligand system. The surface of both frameworks is decorated with pendant -NH_2 and =N-N= functional groups, which makes them to show excellent selectivity for CO_2 among other gases (N_2, O_2, H_2, and Ar). The highest CO_2 adsorption amount was approximately 230 mg/g $_{adsorbent}$ (195 K, 1 atm). Thompson et al. [158] reported the introduction of amine functionality into ZIF-8 through a synthetic approach of introducing 2-aminobenzimidazole as a partial substitution linker to the original 2-methy imidazole.

2. Amine-functionalized MOFs Prepared by Post Synthesis Method

Thus far, amine-functionalized MOFs prepared by a post-synthetic method have been achieved mostly through amine immobilization to the open metal coordination sites of the MOF matrix (Fig. 16). Wang et al. [132] immobilized TEPA on the coordinatively unsaturated Cr (III) sites in MIL-101, which showed excellent CO_2 capture selectivity over CO (70.2 at 25 °C, 0.4 atm). Analysis of the cyclic adsorption performance revealed the high stability of the adsorbent (the adsorbent was regenerated at 100 °C under high vacuum for 1 h). Kim et al. [133] immobilized DETA onto the coordinatively unsaturated Cr sites in MIL-101. They reported a significant decrease in surface area of MIL-101 after DETA grafting, which caused an overall reduction of the CO_2 capture capacity, despite the increased CO_2 adsorption capacity under lower pressure conditions

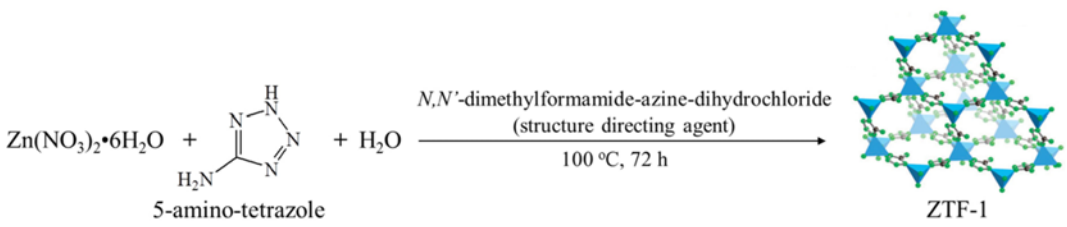

Fig. 15. Synthesis of ZTF-1 [Zn(II), blue; C, black; N, green] [143].

(<15 kpa). Choi et al. [142] modified Mg-MOF-74 by immobilization of its open metal coordination sites with ethylenediamine to introduce pendent amines to the MOF micropores, which increased the CO_2 adsorption capacity under ultra-dilute CO_2 partial pressure conditions. Demessence et al. [152] similarly immobilized ethylenediamine to $H_3[(Cu_4Cl)_3$-$(BTTri)_8]$ MOF with Cu (II) open metal sites, which exhibited a CO_2 uptake of 55 mg/$g_{adsorbent}$ (25 °C, 1 atm), and displayed a very high isosteric heat of adsorption of 90 kJ/mol. Lu et al. [156] reported polyamine-tethered porous polymer networks through the aromatic chloromethylation of the PPN-6 structure and subsequent polyamine substitution. The product, PPN-6-CH_2DETA, exhibited an exceptionally high heat of adsorption (57 kJ/mol) and large adsorption selectivity for CO_2 over N_2 (442). Thompson et al. [158] prepared a ZIF having a mixed linkers and subsequent post-synthetic modication of a mixed-linker ZIF with ethylenediamine, which showed improvement in adsorption selectivity for the CO_2/CH_4 gas pair over ZIF-8 as well as an increase in the heat of adsorption for CO_2.

The incorporation of amine groups into the MOF structure by a post-synthesis method normally leads to a decrease in the surface area and pore volume of the original MOF matrix, which often causes a reduction of the total CO_2 capture capacity after amine incorporation. In addition, the open metal coordination sites of MOF have proven to be effective in CO_2 capture [22,25]. The loss of these active sites after amine incorporation also leads to decrease in CO_2 capture capacity. In this regard, the direct synthesis of an amine-functionalized MOF using an amine-containing ligand may be advantageous in terms of the CO_2 capture capacity. Compared to the original MOFs, the amine-functionalized MOFs exhibited enhanced CO_2 capture selectivity over other gases (such as CH_4, N_2), higher CO_2 uptake in the low pressure regions, and high isosteric heat of adsorption.

CONCLUSIONS AND OUTLOOK

Over the past few decades, a variety of nanoporous materials including mesoporous silica and alumina, zeolite, carbon, porous polymer and MOFs, have been functionalized with amine species for CO_2 capture. This review article provides an overview of the recent advances in such amine-functionalized nanoporous materials as CO_2 adsorbents with an emphasis on their preparation methods and CO_2 capture capacities as well as stability.

Mesoporous silica materials have been studied widely as a support material for amine functionalization through both physical impregnation and chemical grafting methods. A large number of amine moieties can be accommodated inside the mesoporous silica support, leading to a hybrid material with a large CO_2 capture capacity. In addition, the CO_2 capture performance of amine-functionalized mesoporous silica can be improved when water is involved in the adsorption process. These features make amine-functionalized mesoporous silica promising for practical applications in post-combustion CO_2 capture. A few reports involved amine-impregnated mesoporous alumina for CO_2 capture. Amine-impregnated mesoporous alumina show similar CO_2 capture performance to that achieved by amine-impregnated mesoporous silica. The thermal stability of the amine species employed should be considered carefully for long-term implementation. A properly designed mesoporous material with a large pore volume consisting of large mesopores and textural porosity is desirable as a support material.

With regard to microporous materials, such as zeolite, carbon and MOFs, the introduction of amine species to their pore systems through post synthesis normally leads to reduced CO_2 capture capacity, due to a decrease in surface area and pore volume, or the occupation of the open metal sites in MOFs by the amines introduced, but an improvement in CO_2 capture selectivity. Considerable attention has been focused on the direct synthesis of amine-functionalized MOFs using amine-containing ligands as a structural constituent owing to such disadvantages. The hydrothermal stability of the MOFs should be improved significantly for practical implementation. Amine-incorporated MOFs by direct methods can be supplemented further with features such as open metal sites, interpenetration and ion-exchange possibility of the host MOF structures to produce an adsorbent with exceptional CO_2 capture capacity and high CO_2/N_2 or CO_2/CH_4 selectivity. Carbon can emerge as a strong candidate even for amine-grafting because of its abundance, low cost, and surface functionality.

Few studies have examined CO_2 capture by amine-functionalized porous polymers prepared by direct or post synthesis. The synthesis of a porous polymer is growing rapidly and should be exploited more actively to come up with mass-produced and economic CO_2 capturing adsorbents.

ACKNOWLEDGEMENT

This work was supported by a National Research Foundation of Korea (NRF) grant funded by the Korean government (MEST) (No. 2013005862).

REFERENCES

1. A. Yamasaki, *J. Chem. Eng. Jpn.*, **36**(4), 361 (2003).
2. M. Zhao, A. I. Minett and A. T. Harris, *Energy Environ. Sci.*, **6**, 25 (2013).
3. D. M. D'Alessandro, B. Smit and J. R. Long, *Angew. Chem. Int. Ed.*, **49**, 6058 (2010).
4. G. T. Rochelle, *Science*, **325**, 1652 (2009).
5. R. R. Bottoms (Girdler Corp.), US Patent, 1,783,901 (1930).
6. P. D. Vaidya and E. Y. Kenig, *Chem. Eng. Technol.*, **30**, 1467 (2007).
7. A. Veawab, P. Tontiwachwuthikul and A. Chakma, *Ind. Eng. Chem. Res.*, **38**, 3917 (1999).
8. K. P. Resnik, J. T. Yeh and H. W. Pennline, *Int. J. Environ. Technol. Manage.*, **4**(1/2), 89 (2004).
9. G. Rochelle, E. Chen, R. Dugas, B. Oyenakan and F. Seibert, *2005 Annual Conference on Capture and Sequestration*, Alexandria, VA (2006).
10. F. Karadas, M. Atilhan and S. Aparicio, *Energy Fuels*, **24**, 5817 (2010).
11. G. P. Hao, W. C. Li and A. H. Lu, *J. Mater. Chem.*, **21**, 6447 (2011).
12. J. Merel, M. Clausse and F. Meunier, *Environ. Prog.*, **25**, 327 (2006).
13. V. Sebastian, I. Kumakiri, R. Bredesen and M. Menendez, *J. Membr. Sci.*, **292**, 92 (2007).
14. G. Calleja, A. Jimenez, J. Pau, L. Domínguez and P. Pérez, *Gas Sep. Purif.*, **8**, 247 (1994).
15. G. Calleja, J. Pau and J. A. Calles, *J. Chem. Eng. Data*, **43**, 994 (1998).
16. K. S. Walton, M. B. Abney and M. D. Levan, *Micropor. Mesopor.*

Mater., **91**, 78 (2006).
17. E. Dlaz, E. Munoz, A. Vega and S. Ordonez, *Chemosphere*, **70**, 1375 (2008).
18. S. T. Yang, J. Kim and W. S. Ahn, *Micropor. Mesopor. Mater.*, **135**, 90 (2010).
19. R. V. Siriwardane, M. S. Shen, E. P. Fisher and J. A. Poston, *Energy Fuels*, **15**, 279 (2001).
20. B. K. Na, K. K. Koo, H. M. Eum, H. Lee and H. K. Song, *Korean J. Chem. Eng.*, **18**, 220 (2001).
21. J. H. Chen, D. S. H. Wong and C. S. Tan, *Ind. Eng. Chem. Res.*, **36**, 2808 (1997).
22. D. Britt, H. Furukawa, B. Wang, T. G. Glover and O. M. Yaghi, *Proc. Natl. Acad. Sci.*, **106**(49), 20637 (2009).
23. V. Finsy, L. Ma, L. Alaerts, D. E. De Vos, G. V. Baron and J. F. M. Denayer, *Micropor. Mesopor. Mater.*, **120**, 221 (2009).
24. J. An and N. L. Rosi, *J. Am. Chem. Soc.*, **132**, 5578 (2010).
25. L. Grajciar, A. D. Wiersum, P. L. Llewellyn, J. S. Chang and P. Nachtigall, *J. Phys. Chem. C*, **115**, 17925 (2011).
26. L. Hamon, P. L. Llewellyn, T. Devic, A. Ghoufi, G. Clet, V. Guillerm, G. D. Pirngruber, G. Maurin, C. Serre, G. Driver, W. Beek, E. Jolimaître, A. Vimont, M. Daturi and G. Férey, *J. Am. Chem. Soc.*, **131**, 17490 (2009).
27. A. R. Millward and O. M. Yaghi, *J. Am. Chem. Soc.*, **127**, 17998 (2005).
28. C. Chen, J. Kim, D. A. Yang and W. S. Ahn, *Chem. Eng. J.*, **168**, 1134 (2011).
29. Y. Ding and E. Alpay, *Chem. Eng. Sci.*, **55**, 3461 (2000).
30. Y. Liang, D. P. Harrison, R. P. Gupta, D. A. Green and W. J. McMichael, *Energy Fuels*, **18**, 569 (2004).
31. H. Gupta and L. S. Fan, *Ind. Eng. Chem. Res.*, **41**, 4035 (2002).
32. H. Lu, E. P. Reddy and P. G. Smirniotis, *Ind. Eng. Chem. Res.*, **45**, 3944 (2006).
33. N. H. Florin and A. T. Harris, *Chem. Eng. Sci.*, **63**, 287 (2008).
34. N. H. Florin and A. T. Harris, *Chem. Eng. Sci.*, **64**, 187 (2009).
35. J. D. Figueroa, T. Fout, S. Plasynski, H. McIlvried and R. D. Srivastava, *Int. J. Greenhouse Gas Control*, **2**, 9 (2008).
36. Q. Wang, J. Luo, Z. Zhong and A. Borgna, *Energy Environ. Sci.*, **4**, 42 (2011).
37. N. Gargiulo, F. Pepe and D. Caputo, *J. Nanosci. Nanotechnol.*, **14**, 1 (2014).
38. J. R. Li, Y. Ma, M. C. McCarthy, J. Sculley, J. Yu, H. K. Jeong, P. B. Balbuena and H. C. Zhou, *Coord. Chem. Rev.*, **255**, 1791 (2011).
39. K. B. Lee, M. G. Beaver, H. S. Caram and S. Sircar, *Ind. Eng. Chem. Res.*, **47**, 8048 (2008).
40. S. H. Wu, C. Y. Mou and H. P. Lin, *Chem. Soc. Rev.*, **42**, 3862 (2013).
41. C. Gérardin, J. Reboul, M. Bonne and B. Lebeau, *Chem. Soc. Rev.*, **42**, 4217 (2013).
42. T. Asefa and Z. Tao, *Can. J. Chem.*, **90**, 1015 (2012).
43. X. Xu, C. Song, J. M. Andresen, B. G. Miller and A. W. Scaroni, *Micropor. Mesopor. Mater.*, **62**, 29 (2003).
44. X. Xu, C. Song, J. M. Andresen, B. G. Miller and A. W. Scaroni, *Energy Fuels*, **16**, 1463 (2002).
45. X. Xu, C. Song, B. G. Miller and A. W. Scaroni, *Ind. Eng. Chem. Res.*, **44**, 8113 (2005).
46. M. R. Mello, D. Phanon, G. Q. Silveira, P. L. Llewellyn and C. M. Ronconi, *Micropor. Mesopor. Mater.*, **143**, 174 (2011).
47. H. Zhao, J. Hu, J. Wang, L. Zhou and H. Liu, *Acta Phys. Chim. Sinica*, **23**(6), 801 (2007).
48. C. Schumacher, J. Gonzalez, M. Perez-Mendoza, P. A. Wright and N. A. Seaton, *Ind. Eng. Chem. Res.*, **45**, 5586 (2006).
49. M. N. Barbosa, A. S. Araujo, L. P. F. C. Galvao, E. F. B. Silva, A. G. D. Santos, G. E. Luz Jr. and V. J. Fernandes Jr., *J. Therm. Anal. Calorim.*, **106**, 779 (2011).
50. R. S. Franchi, P. J. E. Harlick and A. Sayari, *Ind. Eng. Chem. Res.*, **44**, 8007 (2005).
51. A. Heydari-Gorji, Y. Belmabkhout and A. Sayari, *Langmuir*, **27**, 12411 (2011).
52. P. J. E. Harlick and A. Sayari, *Ind. Eng. Chem. Res.*, **46**, 446 (2007).
53. J. Wei, L. Liao, Y. Xiao, P. Zhang and Y. Shi, *J. Environ. Sci.*, **22**(10), 1558 (2010).
54. M. B. Yue, L. B. Sun, Y. Cao, Y. Wang, Z. J. Wang and J. H. Zhu, *Chem. Eur. J.*, **14**, 3442 (2008).
55. H. Y. Huang, R. T. Yang, D. Chinn and C. L. Munson,. *Ind. Eng. Chem. Res.*, **42**, 2427 (2003).
56. S. Kim, J. Ida, V. V. Guliants and J. Y. S. Lin, *J. Phys. Chem. B*, **109**, 6287 (2005).
57. M. Bhagiyalakshmi, L. J. Yun, R. Anuradha and H. T. Jang, *J. Hazard. Mater.*, **175**, 928 (2010).
58. X. Yan, L. Zhang, Y. Zhang, G. Yang and Z. Yan, *Ind. Eng. Chem. Res.*, **50**, 3220 (2011).
59. R. Sanz, G. Calleja, A. Arencibia and E. S. Sanz-Pérez, *Appl. Surf. Sci.*, **256**, 5323 (2010).
60. A. Heydari-Gorji, Y. Yang and A. Sayari, *Energy Fuels*, **25**, 4206 (2011).
61. L. Wang and R. T. Yang, *J. Phys. Chem. C*, **115**, 21264 (2011).
62. V. Zelenak, M. Badanicova, D. Halamova, J. Čejka, A. Zukal, N. Murafa and G. Goerigk, *Chem. Eng. J.*, **144**, 336 (2008).
63. F. Zheng, D. N. Tran, B. J. Busche, G. E. Fryxell, R. S. Addleman, T. S. Zemanian and C. L. Aardahl, *Ind. Eng. Chem. Res.*, **44**(9), 3099 (2005).
64. N. Hiyoshi, K. Yogo and T. Yashima, *Micropor. Mesopor. Mater.*, **84**, 357 (2005).
65. F. Y. Chang, K. J. Chao, H. H. Cheng and C. S. Tan, *Sep. Purif. Technol.*, **70**, 87 (2009).
66. S. Choi, J. H. Drese, P. M. Eisenberger and C. W. Jones, *Environ. Sci. Technol.*, **45**, 2420 (2011).
67. J. C. Hicks, J. H. Drese, D. J. Fauth, M. L. Gray, G. Qi and C. W. Jones, *J. Am. Chem. Soc.*, **130**, 2902 (2008).
68. W. Chaikittisilp, J. D. Lunn, D. F. Shantz and C. W. Jones, *Chem. Eur. J.*, **17**, 10556 (2011).
69. X. Ma, X. Wang and C. Song, *J. Am. Chem. Soc.*, **131**, 5777 (2009).
70. M. B. Yue, Y. Chun, Y. Cao, X. Dong and J. H. Zhu, *Adv. Funct. Mater.*, **16**, 1717 (2006).
71. J. Wei, J. Shi, H. Pan, W. Zhao, Q. Ye and Y. Shi, *Micropor. Mesopor. Mater.*, **116**, 394 (2008).
72. C. Knofel, J. Descarpentries, A. Benzaouia, V. Zelenak, S. Mornet, P. L. Llewellyn and V. Hornebecq, *Micropor. Mesopor. Mater.*, **99**, 79 (2007).
73. V. Zelenak, D. Halamova, L. Gaberova, E. Bloch and P. Llewellyn, *Micropor. Mesopor. Mater.*, **116**, 358 (2008).
74. C. Chen, W. J. Son, K. S. You, J. W. Ahn and W. S. Ahn, *Chem. Eng. J.*, **161**, 46 (2010).
75. G. P. Knowles, J. V. Graham, S. W. Delaney and A. L. Chaffee, *Fuel Process. Technol.*, **86**, 1435 (2005).

76. G. P. Knowles, S. W. Delaney and A. L. Chaffee, *Ind. Eng. Chem. Res.*, **45**, 2626 (2006).
77. Y. Liu, Q. Ye, M. Shen, J. Shi, J. Chen, H. Pan and Y. Shi, *Environ. Sci. Technol.*, **45**, 5710 (2011).
78. W. J. Son, J. S. Choi and W. S. Ahn, *Micropor. Mesopor. Mater.*, **113**, 31 (2008).
79. C. Chen, S. T. Yang, W. S. Ahn and R. Ryoo, *Chem. Commun.*, 3627 (2009).
80. J. J. Wen, F. N. Gu, F. Wei, Y. Zhou, W. G. Lin, J. Yang, J. Y. Yang, Y. Wang, Z. G. Zou and J. H. Zhu, *J. Mater. Chem.*, **20**, 2840 (2010).
81. D. J. N. Subagyono, Z. Liang, G. P. Knowles and A. L. Chaffee, *Chem. Eng. Res. Des.*, **89**, 1647 (2011).
82. X. Yan, L. Zhang, Y. Zhang, K. Qiao, Z. Yan and S. Komarneni, *Chem. Eng. J.*, **168**, 918 (2011).
83. X. Feng, G. Hu, X. Hu, G. Xie, Y. Xie, J. Lu and M. Luo, *Ind. Eng. Chem. Res.*, **52**, 4221 (2013).
84. W. Li, P. Bollini, S. A. Didas, S. Choi, J. H. Drese and C. W. Jones, *ACS Appl. Mater. Interfaces*, **2**(11), 3363 (2010).
85. W. Yan, J. Tang, Z. Bian, J. Hu and H. Liu, *Ind. Eng. Chem. Res.*, **51**, 3653 (2012).
86. S. H. Liu, C. H. Wu, H. K. Lee and S. B. Liu, *Top. Catal.*, **53**, 210 (2010).
87. N. Hiyoshi, K. Yogo and T. Yashima, *Chem. Lett.*, **37**(12), 1266 (2008).
88. D. Lee, Y. Jin, N. Jung, J. Lee, J. Lee, Y. S. Jeong and S. Jeon, *Environ. Sci. Technol.*, **45**, 5704 (2011).
89. D. S. Dao, H. Yamada and K. Yogo, *Ind. Eng. Chem. Res.*, **52**, 13810 (2013).
90. O. Leal, C. Bolivar, C. Ovalles, J. J. Garcia and Y. Espidel, *Inorg. Chim. Acta*, **240**, 183 (1995).
91. A. Goeppert, M. Czaun, R. B. May, G. K. S. Prakash, G. A. Olah and S. R. Narayanan, *J. Am. Chem. Soc.*, **133**, 20164 (2011).
92. M. Czaun, A. Goeppert, R. B. May, D. Peltier, H. Zhang, G. K. S. Prakash and G. A. Olah, *J. CO_2 Utilization*, **1**, 1 (2013).
93. S. Cui, W. Cheng, X. Shen, M. Fan, A. Russell (Ted), Z. Wu and X. Yi, *Energy Environ. Sci.*, **4**, 2070 (2011).
94. Y. Li, X. Wen, L. Li, F. Wang, N. Zhao, F. Xiao, W. Wei and Y. Sun, *J. Sol-Gel Sci. Technol.*, **66**, 353 (2013).
95. F. Q. Liu, L. Wang, Z. G. Huang, C. Q. Li, W. Li, R. X. Li and W. H. Li, *ACS Appl. Mater. Interfaces*, **6**, 4371 (2014).
96. A. D. Ebner, M. L. Gray, N. G. Chisholm, Q. T. Black, D. D. Mumford, M. A. Nicholson and J. A. Ritter, *Ind. Eng. Chem. Res.*, **50**, 5634 (2011).
97. E. R. Monazam, L. J. Shadle, D. C. Miller, H. W. Pennline, D. J. Fauth, J. S. Hoffman and M. L. Gray, *AIChE J.*, **59**(3), 923 (2013).
98. Y. Tang and K. Landskron, *J. Phys. Chem. C*, **114**, 2494 (2010).
99. M. L. Gray, Y. Soong, K. J. Champagne, H. Pennline, J. P. Baltrus, R. W. Stevens Jr., R. Khatri, S. S. C. Chuang and T. Filburn, *Fuel Process. Technol.*, **86**, 1449 (2005).
100. S. N. Kim, W. J. Son, J. S. Choi and W. S. Ahn, *Micropor. Mesopor. Mater.*, **115**, 497 (2008).
101. S. Araki, H. Doi, Y. Sano, S. Tanaka and Y. Miyake, *J. Colloid Interface Sci.*, **339**, 382 (2009).
102. G. Zhao, B. Aziz and N. Hedin, *Appl. Energy*, **87**, 2907 (2010).
103. G. Qi, Y. Wang, L. Estevez, X. Duan, N. Anako, A. H. A. Park, W. Li, C. W. Jones and E. P. Giannelis, *Energy Environ. Sci.*, **4**, 444 (2011).
104. K. M. Li, J. G. Jiang, S. C. Tian, X. J. Chen and F. Yan, *J. Phys. Chem. C*, **118**, 2454 (2014).
105. S. Yang, L. Zhan, X. Xu, Y. Wang, L. Ling and X. Feng, *Adv. Mater.*, **25**, 2130 (2013).
106. Y. G. Ko, H. J. Lee, H. C. Oh and U. S. Choi, *J. Hazard. Mater.*, **250-251**, 53 (2013).
107. S. Che, A. E. Garcia-Bennett, T. Yokoi, K. Sakamoto, H. Kunieda, O. Terasaki and T. Tatsumi, *Nat. Mater.*, **2**, 801 (2003).
108. C. Chen and W. S. Ahn, *Chem. Eng. J.*, **166**, 646 (2011).
109. W. Chaikittisilp, H. J. Kim and C. W. Jones, *Energy Fuels*, **25**, 5528 (2011).
110. M. G. Plaza, C. Pevida, B. Arias, J. Fermoso, A. Arenillas, F. Rubiera and J. J. Pis, *J. Therm. Anal. Calorim.*, **92**(2), 601 (2008).
111. P. D. Jadhav, R. V. Chatti, R. B. Biniwale, N. K. Labhsetwar, S. Devotta and S. S. Rayalu, *Energy Fuels*, **21**, 3555 (2007).
112. R. Chatti, A. K. Bansiwal, J. A. Thote, V. Kumar, P. Jadhav, S. K. Lokhande, R. B. Biniwale, N. K. Labhsetwar and S. S. Rayalu, *Micropor. Mesopor. Mater.*, **121**, 84 (2009).
113. F. Su, C. Lu, S. C. Kuo and W. Zeng, *Energy Fuels*, **24**, 1441 (2010).
114. X. Xu, X. Zhao, L. Sun and X. Liu, *J. Nat. Gas Chem.*, **18**, 167 (2009).
115. J. Y. Kim, J. Kim, S. T. Yang and W. S. Ahn, *Fuel*, **108**, 515 (2013).
116. S. T. Yang, J. Y. Kim, J. Kim and W. S. Ahn, *Fuel*, **97**, 435 (2012).
117. A. Zukal, I. Dominguez, J. Mayerov and J. Cejka, *Langmuir*, **25**(17), 10314 (2009).
118. L. Zhao, Z. Bacsik, N. Hedin, W. Wei, Y. Sun, M. Antonietti and M. M. Titirici, *Chem Sus Chem*, **3**, 840 (2010).
119. F. Su, C. Lu and H. S. Chen, *Langmuir*, **27**, 8090 (2011).
120. F. Su, C. Lu, W. Cnen, H. Bai and J. F. Hwang, *Sci. Total Environ.*, **407**, 3017 (2009).
121. E. P. Dillon, C. A. Crouse and A. R. Barron, *ACS Nano*, **2**(1), 156 (2008).
122. M. V. M. Mercedes, Z. Lu, Y. Zhang and Z. Tang, *Waste Manage.*, **28**, 2320 (2008).
123. M. L. Gray, Y. Soong, K. J. Champagne, J. Baltrus, R. W. Stevens Jr, P. Toochinda and S. S. C. Chuang, *Sep. Purif. Technol.*, **35**, 31 (2004).
124. M. G. Plaza, C. Pevida, A. Arenillas, F. Rubiera and J. J. Pis, *Fuel*, **86**, 2204 (2007).
125. C. Chen, J. Kim and W. S. Ahn, *Fuel*, **95**, 360 (2012).
126. V. Guillerm, Ł. J. Weseliński, M. Alkordi, M. I. H. Mohideen, Y. Belmabkhout, A. J. Cairns and M. Eddaoudi, *Chem. Commun.*, **50**, 1937 (2014).
127. C. Gebald, J. A. Wurzbacher, P. Tingaut, T. Zimmermann and A. Steinfeld, *Environ. Sci. Technol.*, **45**, 9101 (2011).
128. C. C. Aquino, G. Richner, M. C. Kimling, D. Chen, G. Puxty, P. H. M. Feron and R. A. Caruso, *J. Phys. Chem. C*, **117**, 9747 (2013).
129. C. Chen, D. W. Park and W. S. Ahn, *Appl. Surf. Sci.*, **283**, 699 (2013).
130. M. G. Schwab, B. Fassbender, H. W. Spiess, A. Thomas, X. Feng and K. Müllen, *J. Am. Chem. Soc.*, **131**, 7216 (2009).
131. Y. Lin, C. Kong and L. Chen, *RSC Adv.*, **2**, 6417 (2012).
132. X. Wang, H. Li and X. J. Hou, *J. Phys. Chem. C*, **116**, 19814 (2012).
133. S. N. Kim, S. T. Yang, J. Kim, J. E. Park and W. S. Ahn, *CrystEngComm*, **14**, 4142 (2012).

134. P. Serra-Crespo, E. V. Ramos-Fernandez, J. Gascon and F. Kapteijn, *Chem. Mater.*, **23**, 2565 (2011).
135. S. Couck, J. M. Denayer, G. V. Baron, T. Rémy, J. Gascon and F. Kapteijn, *J. Am. Chem. Soc.*, **131**, 6326 (2009).
136. E. Stavitski, E. A. Pidko, S. Couck, T. Remy, E. J. M. Hensen, B. M. Weckhuysen, J. Denayer, J. Gascon and F. Kapteijn, *Langmuir*, **27**, 3970 (2011).
137. J. Kim, W. Y. Kim and W. S. Ahn, *Fuel*, **102**, 574 (2012).
138. H. R. Abid, J. Shang, H. M. Ang and S. Wang, *Int. J. Smart Nano Mater.*, **iFirst**, 1 (2012).
139. X. Si, C. Jiao, F. Li, J. Zhang, S. Wang, S. Liu, Z. Li, L. Sun, F. Xu, Z. Gabelica and C. Schick, *Energy Environ. Sci.*, **4**, 4522 (2011).
140. B. Arstad, H. Fjellvåg, K. O. Kongshaug, O. Swang and R. Blom, *Adsorption*, **14**, 755 (2008).
141. B. Yuan, D. Ma, X. Wang, Z. Li, Y. Li, H. Liu and D. He, *Chem. Commun.*, **48**, 1135 (2012).
142. S. Choi, T. Watanabe, T. H. Bae, D. S. Sholl and C. W. Jones, *J. Phys. Chem. Lett.*, **3**, 1136 (2012).
143. T. Panda, P. Pachfule, Y. Chen, J. Jiang and R. Banerjee, *Chem. Commun.*, **47**, 2011 (2011).
144. T. M. McDonald, W. R. Lee, J. A. Mason, B. M. Wiers, C. S. Hong and J. R. Long, *J. Am. Chem. Soc.*, **134**, 7056 (2012).
145. B. Zheng, J. Bai, J. Duan, L. Wojtas and M. J. Zaworotko, *J. Am. Chem. Soc.*, **133**, 748 (2011).
146. C. Montoro, E. Garc, S. Calero, M. A. Perez-Fernandez, A. L. Lopez, E. Barea and J. A. R. Navarro, *J. Mater. Chem.*, **22**, 10155 (2012).
147. N. Ko and J. Kim, *Bull. Korean Chem. Soc.*, **32**(8), 2705 (2011).
148. Z. Xiang, S. Leng and D. Cao, *J. Phys. Chem. C*, **116**, 10573 (2012).
149. J. Duan, Z. Yang, J. Bai, B. Zheng, Y. Li and S. Li, *Chem. Commun.*, **48**, 3058 (2012).
150. Q. G. Zhai, Q. Lin, T. Wu, L. Wang, S. T. Zheng, X. Bu and P. Feng, *Chem. Mater.*, **24**, 2624 (2012).
151. T. M. McDonald, D. M. D'Alessandro, R. Krishna and J. R. Long, *Chem. Sci.*, **2**, 2022 (2011).
152. A. Demessence, D. M. D'Alessandro, M. L. Foo and J. R. Long, *J. Am. Chem. Soc.*, **131**, 8784 (2009).
153. R. Vaidhyanathan, S. S. Iremonger, K. W. Dawson and G. K. H. Shimizu, *Chem. Commun.*, 5230 (2009).
154. J. An, S. J. Geib and N. L. Rosi, *J. Am. Chem. Soc.*, **132**, 38 (2010).
155. R. Vaidhyanathan, S. S. Iremonger, G. K. H. Shimizu, P. G. Boyd, S. Alavi and T. K. Woo, *Science*, **330**, 650 (2010).
156. W. Lu, J. P. Sculley, D. Yuan, R. Krishna, Z. Wei and H. C. Zhou, *Angew. Chem. Int. Ed.*, **51**, 7480 (2012).
157. R. Haldar, S. K. Reddy, V. M. Suresh, S. Mohapatra, S. Balasubramanian and T. K. Maji, *Chem. Eur. J.*, **20**, 4347 (2014).
158. J. A. Thompson, N. A. Brunelli, R. P. Lively, J. R. Johnson, C. W. Jones and S. Nair, *J. Phys. Chem. C*, **117**, 8198 (2013).